Colloid Polym Sci 278:137–142 (2000)


ORIGINAL CONTRIBUTION

R. Beck
M. Gradzielski
K. Horbaschek
S.S. Shah
H. Hoffmann
P. Strunz

# Phase behaviour and physical properties of the cationic quaternary system tetradecyldimethylamine oxide hydrochloric acid 1-hexanol water

Received: 11 July 1999
Accepted: 25 August 1999

Presented at the 39th General Meeting of the Kolloid-Gesellschaft, Würzburg, 27–30 September 1999

R. Beck (✉) · M. Gradzielski
K. Horbaschek · S.S. Shah · H. Hoffmann
Lehrstuhl für Physikalische Chemie I
Universität Bayreuth D-95440 Bayreuth
Germany
e-mail: Reiner.Beck@uni-bayreuth.de
Tel.: +49-921-552765

P. Strunz
Hahn-Meitner-Institut
Glienicker Strasse 100
D-14109 Berlin, Germany

S.S. Shah
Department of Chemistry
Quaid-i-Azam University
Islamabad 45320, Pakistan

**Abstract** The phase behaviour and properties of the tetradecyldimethylamine oxide/HCl/hexanol/water quaternary surfactant system have been studied by means of electric conductivity, rheology, freeze-fracture transmission electron microscopy (FF-TEM) and small-angle neutron scattering (SANS). In this system the originally zwitterionic surfactant can become increasingly charged by protonation through the addition of HCl, i.e. the degree of charging can be changed continuously. An interesting, isotropic phase ($L_1^*$ phase) of low viscosity was observed for intermediate degrees of charging. From viscosity and conductivity measurements this phase can clearly be distinguished from the conventional $L_1$ phase that is composed of micelles. Investigation of the structures present by means of FF-TEM and SANS showed that the $L_1^*$ phase is made up of unilamellar vesicles of extremely small diameter of 8–10 nm. Evidently such highly curved structures are stabilized by the electrostatic conditions in this system.

**Key words** Small vesicles · Phase behaviour · Small-angle neutron scattering · Charged surfactants

## Introduction

In many investigations the influence of the charge density on the critical micelle concentration (cmc), the aggregation number of the micelles, the phase boundaries and the structural transformation has been studied [1–3]. The shielding of electrostatic repulsion between charged headgroups results in more densely packed surfactant molecules at interfaces. This lowers the cmc and can lead to phase transitions and the formation of bilayer-type structures [4].

Several types of bilayer phases exist in surfactant *n*-alcohol water systems [5]. The influence of ionic charges on the phase behaviour of the zwitterionic surfactant tetradecyldimethylamine oxide (TDMAO) with alcohols as cosurfactants has been reported in previous papers [5–7], such as in the case of TDMAO which was gradually replaced by cationic tetradecyltrimethylammonium bromide (TTMABr) [6, 7] or anionic sodium dodecyl sulfate [18]. In these charged systems, the phase diagram becomes simpler than in the uncharged system. With increasing hexanol one finds a wider micellar phase ($L_1$), a two-phase region ($L_1 + L_\alpha$) and a lamellar $L_\alpha$ phase.

In this investigation the TDMAO/hexanol/water system was charged by addition of HCl. By protonation of the amine oxide group

$$C_{14}H_{29}\text{-}N(CH_3)_2\text{-}O + HCl \rightarrow C_{14}H_{29}\text{-}N(CH_3)_2\text{-}O\text{-}H^+ + Cl^-$$

one obtains a mixture of charged and uncharged surfactants that have the same chain length and a

basically identical chemical structure. We studied the sequence of phases of the system and discovered an interesting low viscosity, isotropic phase that appears inside the two-phase $L_1/L_\alpha$ region. The properties of this phase and the structures present were studied by means of conductivity measurements, rheology, small-angle neutron scattering (SANS) and freeze-fracture transmission electron microscopy (FF-TEM).

## Materials and methods

The TDMAO was a gift from Clariant, Gendorf, and was recrystallized twice from acetone. 1-Hexanol from Fluka and 0.5 N HCl solution from Merck were both of p.a. quality and were used without further purification.

Conductivity measurements were performed with a conductivity bridge (Wayne Kerr B90) and a glass electrode (WTW, LTA/S) calibrated with a 10 mM KCl solution. The surfactant solution was put in a thermostated bottle and the required amount of hexanol was added using a micropipette (Pipetman P). All measurements were made at 25 °C. To guarantee the homogeneity of the solution, it was stirred for 10 min, and measurements were made while the solution was stirred.

The viscosities of the low-viscosity samples were measured using an oscillating capillary rheo- and densitymeter (OCR-D) from Chempro AP PAAR at a frequency of 2 Hz. A Bohlin CS 10 stress-controlled rheometer and a Rheometer RFR 7800 strain-controlled rheometer were also used for measurements of the high-viscosity phases. The viscoelastic properties, i.e. the dynamic modulus and the magnitude of the complex viscosity, were determined by dynamic measurements from 0.01 to 100 rad/s.

FF-TEM was performed with a CEM 902 EM from Zeiss. A small amount of the sample was sandwiched between two 0.1-mm-thick copper discs and was frozen by plunging it in liquid propane, which was cooled with liquid nitrogen. Fracturing and replication were carried out in a FF apparatus (BAF 400 freeze etching system) at a temperature of −140 °C. At an angle of 45° the sample was deposited with Pt/C.

SANS experiments were performed at the Hahn-Meitner-Institut in Berlin on the V4 SANS instrument. The scattering intensity was recorded on a 64 × 64 two-dimensional $^3$He detector. The distances between the sample and the detector were 1, 4 and 15.85 m. The neutrons for the experiment were selected using a mechanical velocity selector with a distribution of wavelengths of 10% fullwidth at half-maximum. The wavelength employed was 0.6 nm. The samples were contained in Helma quartz cuvettes of 1- or 2-mm thickness and a $q$ range of 0.04–4 nm$^{-1}$ was covered in the experiments.

## Results and discussion

### Phase behaviour

Solutions of TDMAO/hexanol/water show the typical phase behaviour of a surfactant/cosurfactant system with several bilayer phases. The phase behaviour of this system has been studied before [6]. It has been shown that by charging the system, for example, by admixture of TTMABr, the phase diagram becomes much simpler. The $L_{\alpha h}$ and $L_3$ phases disappear and only a $L_1$ and $L_{\alpha l}$ region exists in this system [6].

In analogy to the TDMAO/TTMABr/hexanol/water quaternary system the phase sequence of the TDMAO/HCl/hexanol/water quaternary system was established for a constant surfactant concentration of 100 mM and is shown in Fig. 1 as a function of the concentration of HCl and 1-hexanol at 25 °C. The surfactant becomes protonated by HCl since the effective p$K_a$ of $TDMAOH^+$ is around 4.9 [9], which means that practically all protons bind to TDMAO. The sequence of the different mesophases in the uncharged ternary system is schematically written along the $y$-axis of the diagram.

With increasing hexanol content one finds that the isotropic $L_1$ phase is followed by an extended $L_1/L_{\alpha l}$ two-phase region. The micellar $L_1$ phase extends to higher hexanol levels with increasing content of HCl. A clear $L_{\alpha l}$ phase is only observed at HCl contents less than 40 mM and it exists for hexanol concentrations between 120 and 380 mM. Above this hexanol concentration, the $L_{\alpha l}$ phase disappears and an alcohol-rich, milky two-phase area is found, which does not phase-separate macroscopically. In systems containing more than 30 mM HCl (corresponding to 30% charged surfactant) no monophasic $L_{\alpha l}$ phase is observed.

However, the most interesting part of this phase diagram is the small isotropic $L_1^*$ phase (it is called $L_1^*$ here since it is clearly separated in the phase diagram from the normal $L_1$ phase, and is clearly distinguishable by its properties as shown later), which is completely surrounded by the two-phase region. The concentration range for this $L_1^*$ phase is very small and lies between 40 and 50 mM HCl and 110 and 120 mM hexanol. The phase is transparent, of low viscosity and isotropic, and it will be shown later that it contains extremely small

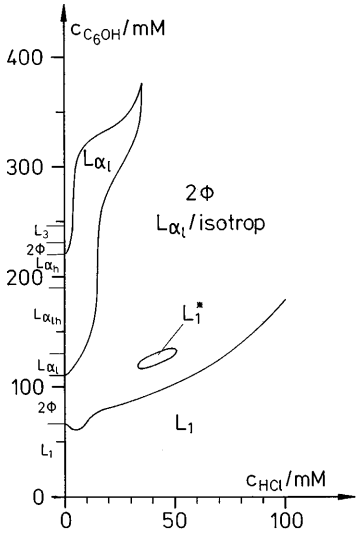


**Fig. 1** Phase diagram of the tetradecyldimethylamine oxide (TDMAO)/HCl/1-hexanol/water system. The total surfactant concentration was kept constant at 100 mM and the concentrations of HCl and hexanol were varied. The sequence of the different mesophases in the uncharged system is shown schematically on the *left side* of the diagram

unilamellar vesicles. It is stable over fairly long periods of time and does not change appreciably during this time; however, after several months a small turbid layer was observed to develop at the top of the samples.

To extend the phase diagram, the concentration of TDMAO was varied from 10 to 120 mM while keeping the relative amount of charged surfactant constant at 40 mol%. The phase diagram of this system with different surfactant concentrations and a constant degree of charging is shown in Fig. 2. One observes that the $L_1^*$ phase for concentrations between 75 and 105 mM TDMAO is separated from the $L_1$ phase by a two-phase region. The phase boundary between the $L_1$ phase and the $L_1/L_{\alpha l}$ two-phase region is almost constant and moves with increasing TDMAO concentrations to higher cosurfactant concentrations. At lower surfactant concentrations the phase boundary between $L_1$ and $L_1/L_{\alpha l}$ is at a much higher concentration. In this region the transition between $L_1$ and $L_1^*$ takes place seemingly without passing through a $L_1/L_{\alpha l}$ two-phase region. This region is directly connected to the $L_1^*$ region, which extends into the two-phase $L_1/L_\alpha$ region at higher surfactant concentrations. Therefore it is actually possible that the $L_1^*$ phase is really a two-phase region that looks like an $L_1$ phase but is metastable. The phase boundary between $L_1$ and $L_1^*$ was determined by conductivity measurements and is shown in Fig. 2 as a dashed line.

Finally at surfactant concentrations above 110 mM and at fairly high hexanol concentrations (about 400 mM) a clear lamellar $L_{\alpha l}$ phase is observed with a yield stress. Evidently by charging up the system the stability range of the $L_{\alpha l}$ phase has been shifted to higher total surfactant concentrations.

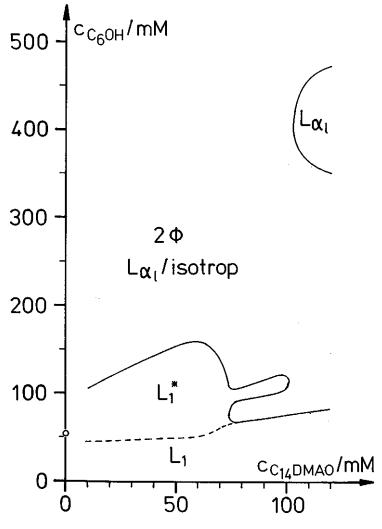


**Fig. 2** Phase diagram of the TDMAO/HCl/1-hexanol/water system. The surfactant and cosurfactant concentrations were varied and the degree of charging was kept constant at 40%, i.e. $c$(HCl) = 0.4 $c$(TDMAO)

## Electric conductivity

It is well known that the electrical conductivity of a charged vesicle solution is significantly lower than that of a micellar solution [7, 10], and because of this we were able to distinguish between the $L_1$ and the $L_1^*$ phases. For this purpose the corresponding surfactant solutions were titrated with cosurfactant and the results of these measurements are shown in Fig. 3, where the conductivity data of 100 mM TDAMO solution are plotted against hexanol concentration for various HCl concentrations. A similar behaviour of the conductivity values within the $L_1$ phase has been observed before for the alkylamine oxide/TTMABr system [6, 7]. With increasing charge density (TTMABr or HCl content), the conductivity of the $L_1$ phase initially decreases somewhat and then rises with hexanol addition until the $L_1/L_\alpha$ phase boundary is reached. For still higher hexanol concentrations the conductivity decreases markedly (marked with arrows in Fig. 3).

The significant decrease in the conductivity at the $L_1/L_{\alpha l}$ phase boundary is caused by the formation of vesicles. Some of the ions are trapped inside the vesicles and are not able to contribute anymore to the charge transport. For HCl concentrations between 30 and 60 mM the solutions become turbid at the $L_1/L_{\alpha l}$ phase boundary and the conductivity drops sharply by about 30–40%, but then at hexanol concentrations between 100 and 150 mM a plateau of nearly constant conductivity values is reached. This plateau is observed in the transparent, isotropic $L_1^*$ phase. Above concentrations of 150 mM hexanol, the solutions become turbid again and the conductivity decreases until the solutions reach the vesicle phase or the alcohol-rich phase; these phases have constant conductivity.

The constant conductivity in the $L_1^*$ phase means that the concentration of $Cl^-$ counterions, which are respon-

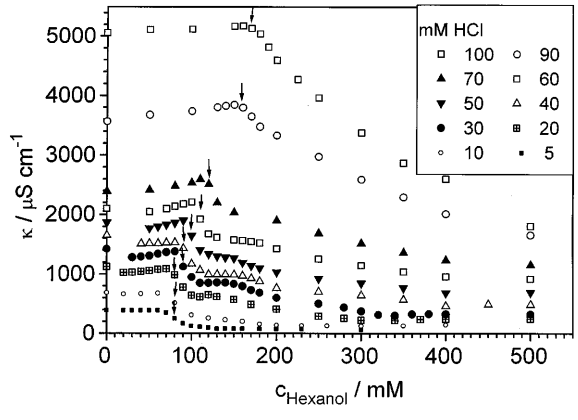


**Fig. 3** Plots of the electric conductivity, $\kappa$, against the hexanol concentration for a constant surfactant concentration of 100 mM with varying content of HCl at 25 °C (the beginning of the $L_1^*$ phase is marked with an *arrow*)

sible for the charge transport, remains at the same level with increasing addition of hexanol. This indicates that the vesicles in this region do not become multilamellar or grow in size, because this should reduce the conductivity. After addition of more hexanol these small vesicles grow again to form big multilamellar vesicles and the conductivity values decrease again.

At surfactant concentrations below 75 mM the $L_1$ and $L_1^*$ phases are not separated macroscopically by a two-phase area. Nevertheless the conductivity measurements prove that a morphological transition from micelles to vesicles occurs. This transition from a clear micellar phase to a clear vesicular phase without observing a two-phase region has been described by Hoffmann et al. [11] and Oberdisse et al. [12].

## Rheological measurements

The zero-shear viscosity, $\eta_0$, for a 100 mM TDMAO and 50 mM hexanol solution is shown in Fig. 4 as a function of the HCl concentration. The relatively viscous surfactant/cosurfactant solution becomes even more viscous after the addition of a small amount of HCl. The uncharged solution forms rodlike micelles. The maximum of the zero-shear viscosity is a result of the stiffening of, and the increased interaction between, these micelles by charging them. The highly viscous samples indicate the formation of an entangled network [8, 13, 14].

With increasing charge density the viscosity is sharply reduced after the maximum of 1200 mPas at 10 mM HCl. This indicates that the rodlike micelles decrease in size with increasing hexanol concentration, the network is destroyed and finally in the fully charged system no rods are found. The reason for this is the repulsion of the charged headgroups on the micelle surface. With rising HCl concentration the repulsion increases and this corresponds to an increasing spontaneous curvature of the surfactant monolayer. As a consequence increasingly more hexanol can now be incorporated into these systems until a limiting lower curvature is reached beyond which no further hexanol can be solubilized. This explains the fact that the $L_1$ phase expands to higher hexanol concentrations with increasing concentrations of HCl (Fig. 1).

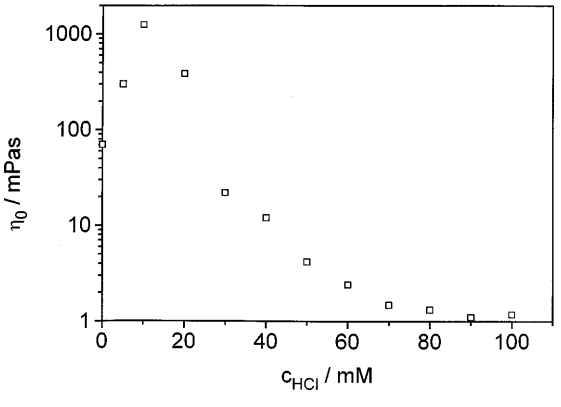


**Fig. 4** Plot of the zero-shear viscosity, $\eta_0$ of the 100 mM TDMAO/50 mM hexanol/HCl system as a function of HCl concentration

The rheological properties of the $L_{\alpha l}$ phase were also investigated. For the whole frequency range $G'$ and $G''$ are almost constant and $G'$ is larger than $G''$ by about 1 order of magnitude. The system possesses a yield stress, i.e. it has no finite structural relaxation time. This yield-stress value disappears for hexanol concentrations higher than 300 mM, where the alcohol-rich two-phase region is entered. With respect to the properties of the $L_{\alpha l}$ phase the TDMAO/HCl/hexanol system resembles the TDMAO/TTMABr/hexanol system which had been investigated in detail before [6].

## Freeze-fracture transmission electron microscopy

The most interesting phase in our system (and one that has not been observed at all in the TDMAO/TTMABr/hexanol system) is the $L_1^*$ phase. In order to determine its microstructure FF-TEM micrographs were obtained for samples of this phase that contained 90 mM TDMAO, 110 mM hexanol and 36 mM HCl (Fig. 5).

In Fig. 5 some large vesicles are seen with radii in the range 70–500 nm. The smaller ones seem to be unilamellar while the bigger ones are multilamellar. While the shape of the smaller vesicles is perfectly round, the big ones seem deformed. On the surface of these vesicles some undulations can be observed, which could be due to the preparation of the replicas. Some of the multilamellar vesicles are cross-fractured and show interlamellar distances of 30–40 nm.

The distance between these vesicles is very large and evidently most of the amphiphilic material has to be present in a different form of aggregation. On closer inspection of the electron micrographs, a large number of small aggregates of about 10-nm diameter can be seen; however, these objects are too small to have their structure well resolved by means of FF-TEM, but it seems that the main part of the amphiphile which is missing by just regarding the larger vesicles has to be assembled in such small structures.

## Small-angle neutron scattering

SANS experiments were performed to investigate in more detail the structure of the small aggregates seen in the electron micrographs . The $q$ range was chosen in such a way as to cover well the interaction peak that is observed in the sample and also the high $q$ region, which should be sensitive to the local curvature of the aggregates observed.

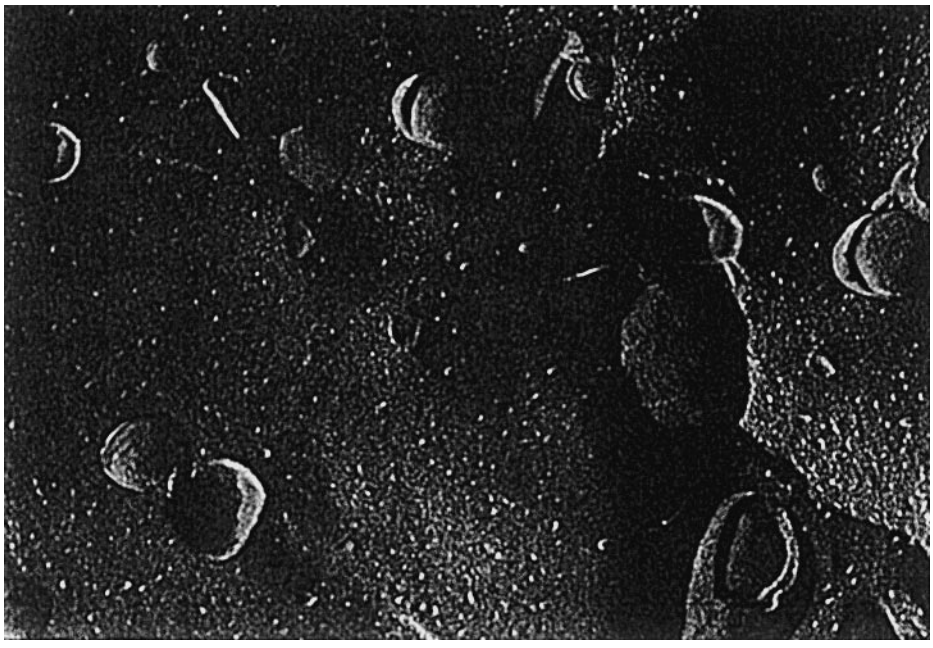


**Fig. 5** Freeze-fracture transmission electron microscopy micrographs of the system containing 90 mM TDMAO/36 m/M/HCl. 110 mM hexanol. The *bars* correspond to 200 nm

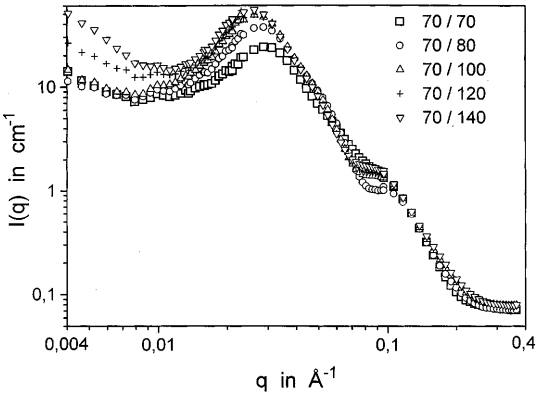


**Fig. 6** Radially averaged small-angle neutron scattering intensity, $I$, as a function of the scattering vector, $q$. The degree of charging was kept constant at 40 mol%. The composition of the samples is given in the *inset*, where the *first number* is the concentration of TDMAO in millimoles and the *second number* is the concentration of hexanol in millimoles. The TDMAO concentration was kept constant and the hexanol concentration was varied

The radially averaged scattering intensity is given for various surfactant and cosurfactant concentrations (all have a degree of charging of 40%) in Fig. 6. All curves look very similar. An interaction peak is located between 0.022 and 0.03 $\text{Å}^{-1}$ and is followed by a flat region or even a shallow minimum around 0.08–0.1 $\text{Å}^{-1}$. At still higher $q$ values the curves are almost superimposed. The similar shape of the curves indicates that the structures present are almost the same for all samples.

For a quantitative evaluation we fitted a model of polydisperse shells to the experimental data. Since an interaction peak is observed in the SANS curves evidently a structure factor, $S(q)$, is required to describe this feature, besides the form factor, $P(q)$. The polydispersity of the average radius, $R$, is given by a Schulz distribution. $R$ is the radius of the vesicles at the middle of the surfactant bilayer. With the variance, $\Delta R$, of the Schulz distribution we can calculate the polydispersity index, $p = \Delta R/R$. The results are summarized in Table 1.

The thickness, $D$, and also $D_{L_\alpha}$ obtained from the high $q$ range are always around 22 Å and decrease slightly with increasing relative hexanol content (see series 70/70–70/140) as one might expect for a bilayer that is increasingly made up of the shorter-chain alcohol. $p$ is always around 0.25–0.3 (except for the 70/70 sample, for which a much smaller radius was also obtained; however, the deviation in that case is due to the fact that this sample is not yet located in the $L_1^*$ phase but is still in the transition region between the $L_1$ phase and the $L_1^*$ phase and therefore still contains a significant number of rodlike micelles, which are responsible for the different scattering behaviour), which means that the vesicles are not extremely monodisperse but that they still possess a

**Table 1** Results of the fits to the small-angle neutron scattering data for samples with a constant tetradecyldimethylamine oxide (*TDMAO*) concentration of 70 mM. The mean shell radius, $R_m$, the thickness of the shells, $D$, the polydispersity index, $p$, the effective charge, $z$, are given

| $c$ (TDMAO/1-hexanol)/mM | 70/70 | 70/80 | 70/100 | 70/120 | 70/140 |
|---|---|---|---|---|---|
| $R_m$/Å | 20.4 | 31.8 | 34.8 | 36.1 | 37.2 |
| $D$/Å | 22.6 | 22.7 | 22.3 | 22.0 | 21.9 |
| $p$ | 0.727 | 0.273 | 0.288 | 0.295 | 0.321 |
| $z/e_0$ | 7.5 | 11.6 | 12.3 | 11.8 | 11.8 |

well-defined size as manifested by the minimum in the SANS curves.

The effective charge of the aggregates also remains almost constant around 12 $e_0$, which for aggregates of the given size means that only about 2.5% of the ionizable headgroups are effectively charged (and the remaining $Cl^-$ ions are condensed at the headgroup or in its vicinity). This value is somewhat lower than those observed for spherical micelles [15, 16]. The more effective counterion binding in our case might be due to the fact that the counterion is $H^+$, which in our system can become even more effectively bound by the formation of hydrogen bonds with neighbouring N-O headgroups.

The SANS experiments clearly demonstrate that the $L_1^*$ phase is primarily composed of small unilamellar vesicles of a diameter of around 8–10 nm, while some larger vesicular aggregates are still present. There is an equilibrium between very small and large vesicles. It might be noted that such coexistence has been argued for on basis of a Poisson–Boltzmann cell model for charged vesicles under certain electrostatic conditions [17]. Such conditions might well be fulfilled in our case.

## Conclusion

We have studied the phase behaviour, the macroscopic properties and the structures present in the TDMAO/HCl/hexanol/water quaternary system. The originally uncharged zwitterionic TDMAO can become charged by protonation with HCl and by this means one can vary continuously the degree of charging of the surfactant. With increasing concentration of HCl we found an expansion of the isotropic phase to higher hexanol concentrations and a large broadening of the $L_1/L_\alpha$ two-phase region. The charging of the system simplifies the phase diagram. The lamellar $L_{\alpha h}$ phase and the $L_3$ phase of the uncharged system are extremely sensitive to electrostatic charges and disappear completely. Even the monophasic vesicular $L_{\alpha 1}$ phase exists only at degrees of charging below 30%.

The most interesting phenomenon is the occurrence of the isotropic $L_1^*$ phase which was observed for intermediate degrees of charging of 30–60%. At higher surfactant concentrations this $L_1^*$ phase is sandwiched between a two-phase $L_1/L_{\alpha 1}$ region, but at lower surfactant concentrations it is directly connected to the micellar $L_1$ phase. By means of FF-TEM and SANS we determined that this phase contains some large multilamellar vesicles of diameter 70–500 nm but that it is mainly composed of small unilamellar vesicles of diameter 8–10 nm.

The distinction between the $L_1$ phase and the $L_1^*$ phase is most easily made by means of conductivity measurements. The transition points are marked by an abrupt decrease in the conductivity upon addition of hexanol, which is due to the formation of vesicular aggregates in which some of the counterions becomes trapped. Within the $L_1^*$ phase the conductivity remains at a constant plateau value. In contrast the $L_{\alpha 1}$ phase exhibits strongly elastic properties and possesses a yield stress. The transition between the micellar $L_1$ phase and $L_1^*$ phase could be observed in both conductivity and rheology experiments, even when no macroscopic two-phase region was observed between the two phases.

**Acknowledgements** We would like to thank the Hahn-Meitner-Institut for financial help with the SANS experiments through the Training and Mobility of Researches (TMR) Large-scale facilities (LSF) contact ERBF MGE CT 950060 of the European Community. S.S. is grateful to the DAAD for financial support. We would also like to thank D. Gräbner and M. Müller for help with the SANS experiments.

## References

1. Jönsson B, Wennerström H (1981) J Colloid Interface Sci 80:482
2. Safran SA, Pincus PA, Cates ME, MacKintosh FC (1990) J Phys 51:503
3. Hoffmann H (1990) Prog Colloid Polym Sci 83:16
4. Hoffmann H, Oetter G, Schwander B (1987) Prog Colloid Polym Sci 73:95
5. Hoffmann H, Thunig C, Schmiedel P, Munkert U (1995) Faraday Discuss 101:319
6. Hoffmann H, Munkert U, Thunig C, Valiente M (1994) J Colloid Interface Sci 163:217
7. Valiente M, Munkert U, Thunig C, Lenz U, Hoffmann H (1993) J Colloid Interface Sci 160:39
8. Platz G, Thunig C, Hoffmann H (1992) Ber Bunsenges Phys Chem 96:667
9. Rathman JF, Scheuning DR (1991) ACS Symp Ser 447:123
10. Hervé P, Roux D, Bellocq AM, Nallet F, Gulik-Krzywicki T (1993) J Phys II 3:1255
11. Hoffmann H, Thunig C, Schmiedel P, Munkert U (1994) Langmuir 10:3972
12. Oberdisse J, Couve C, Appell J, Berret JF, Ligoure C, Porte G (1996) Langmuir 12:1212
13. Brye TJ, Cates ME (1992) J Chem Phys 96:1367
14. Candau J, Khatory A, Lequeux F, Kern F (1993) J Phys IV 3:197
15. Gorski N, Gradzielski M, Hoffmann H (1994) Langmuir 10:2594
16. Bucci S, Fagotti C, Degiorgio V, Piazza R (1991) Langmuir 7:824
17. Oberdisse J (1998) Eur Phys J B 3:463
18. Illner J-C (1995) Dissertation Universität Bayreuth